Donor Heterogeneity in the Human Macrophage Response to a Biomaterial under Hyperglycemia in vitro

TISSUE ENGINEERING: Part C
Volume 28, Number 8, 2022

DOI: 10.1089/ten.tec.2022.0066

termis
Tissue Engineering
& Regenerative Medicine
International Society

Open camera or QR reader and scan code to access this article and other resources online.

SPECIAL ISSUE: IMMUNOMODULATORY METHODS TOWARD TISSUE REGENERATION

Donor Heterogeneity in the Human Macrophage Response to a Biomaterial Under Hyperglycemia *In Vitro*

Suzanne E. Koch, PhD,[1,2] Franka L.P. Verhaegh, MSc,[1,2] Simone Smink, BSc,[1,2] Silvia M. Mihăilă, PhD,[3] Carlijn V.C. Bouten, PhD,[1,2] and Anthal I.P.M. Smits, PhD[1,2]

Macrophages have a commanding role in scaffold-driven *in situ* tissue regeneration. Depending on their polarization state, macrophages mediate the formation and remodeling of new tissue by secreting growth factors and cytokines. Therefore, successful outcomes of material-driven *in situ* tissue vascular tissue engineering depend largely on the immuno-regenerative potential of the recipient. A large cohort of patients requiring vascular replacements suffers from systemic multifactorial diseases, such as diabetes, which gives rise to a hyperglycemic and aggressive oxidative inflammatory environment that is hypothesized to hamper a well-balanced regenerative process. Here, we aimed at fundamentally exploring the effects of hyperglycemia, as one of the hallmarks of diabetes, on the macrophage response to three-dimensional (3D) electrospun synthetic biomaterials for *in situ* tissue engineering, in terms of inflammatory profile and tissue regenerative capacity. To simulate the early phases of the *in situ* regenerative cascade, we used a bottom-up *in vitro* approach. Primary human macrophages ($n = 8$ donors) were seeded in two-dimensional (2D) culture wells and polarized to pro-inflammatory M1 and anti-inflammatory M2 phenotype in normoglycemic (5.5 mM glucose), hyperglycemic (25 mM), and osmotic control (OC) conditions (5.5 mM glucose, 19.5 mM mannitol). Unpolarized macrophages and (myo)fibroblasts were seeded in mono- or co-culture in a 3D electrospun resorbable polycaprolactone bisurea scaffold and exposed to normoglycemic, hyperglycemic, and OC conditions. The results showed that macrophage polarization by biochemical stimuli was effective under all glycemic conditions and that the polarization states dictated expression of the receptors *SCL2A1* (glucose transporter 1) and *CD36* (fatty acid transporter). In 3D, the macrophage response to hyperglycemic conditions was strongly donor-dependent in terms of phenotype, cytokine secretion profile, and metabolic receptor expression. When co-cultured with (myo)fibroblasts, hyperglycemic conditions led to an increased expression of fibrogenic markers (*ACTA2, COL1, COL3, IL-1β).* Together, these findings show that the hyperglycemic and hyperosmotic conditions may, indeed, influence the process of macrophage-driven *in situ* tissue engineering, and that the extent of this is likely to be patient-specific.

Keywords: macrophage polarization, scaffold, tissue engineering, diabetes, vascular graft

Impact Statement

Success or failure of cell-free bioresorbable *in situ* tissue-engineered vascular grafts hinges around the immuno-regenerative response of the recipient. Most patients requiring blood vessel replacements suffer from additional multifactorial diseases,

[1]Department of Biomedical Engineering, Eindhoven University of Technology, Eindhoven, The Netherlands.
[2]Institute for Complex Molecular Systems (ICMS), Eindhoven University of Technology, Eindhoven, The Netherlands.
[3]Division of Pharmacology, Department of Pharmaceutical Sciences, Utrecht University, Utrecht, The Netherlands.

such as diabetes, which may compromise their intrinsic regenerative potential. In this study, we used a bottom-up approach to study the effects of hyperglycemia, a hallmark of diabetes, on important phases in the *in situ* regenerative cascade, such as macrophage polarization and macrophage–myofibroblast crosstalk. The results demonstrate a relatively large donor-to-donor variation, which stresses the importance of taking scaffold-independent patient-specific factors into account when studying *in situ* biomaterial-driven tissue engineering.

Introduction

NUMEROUS STUDIES HAVE shown the preclinical application of resorbable, synthetic scaffolds for the *in situ* regeneration of blood vessels[1–4] and heart valves,[5–7] as well as applications outside the cardiovascular field (e.g., abdominal wall reconstruction[8]). Moreover, clinical trials have demonstrated promising results for the use of such scaffolds in pediatric patients with congenital cardiac malformations.[9–11] Scaffolds for *in situ* tissue regeneration are designed to induce regeneration on implantation, directly at the functional site.

Many aspects underlying *in situ* tissue regeneration remain to be elucidated, but it is hypothesized that its stages mirror the natural wound-healing cascade.[12] On implantation of the scaffold, proteins adhere to the scaffold and form a protein layer, which interacts with blood clotting components to result in a provisional matrix with which recruited cells can interact. During the acute inflammatory phase, neutrophils and monocyte-derived macrophages invade the fibrous graft,[13] and secrete a wide array of cytokines and growth factors, to attract other host immune cells (e.g., T-helper cells) and tissue-producing cells (e.g., [myo]fibroblasts, and progenitor/stem cells).

Macrophages show a tremendous plasticity and can polarize in response to local cues over a continuous spectrum, from pro-inflammatory ''classically activated'' (M1) to pro-regenerative ''alternatively activated'' (M2) phenotypes at the extremes.[14,15] For the *in situ* regenerative response, a timely shift from M1 (day 0–4) to M2 (day 4–7) macrophages is crucial.[15–17] In the resolution phase, the formed tissue should be remodeled resulting in a well-organized functional neo-tissue. Over time, once new tissue is being formed, the synthetic biomaterial can be gradually resorbed *via* hydrolysis and/or oxidation.[12]

Successful integration of *in situ* tissue-engineered constructs largely depends on the immuno-regenerative potential of the recipient.[18,19] This raises the question whether the preclinical and clinical results for *in situ* cardiovascular tissue engineering will also be applicable in more challenging patient cohorts with a compromised immunological and/or regenerative capacity. A large cohort of the patients requiring cardiovascular replacements suffer from systemic multifactorial diseases, such as diabetes, which gives rise to a hyperglycemic and aggressive oxidative inflammatory environment that is hypothesized to hamper a well-balanced regenerative process.

Diabetes is a rising global epidemic. It is estimated that 463 million individuals (aged 20–79 years) suffered from diabetes in 2019, which is expected to increase up to 700 million patients in 2045.[20] This increase in diabetes prevalence goes hand in hand with an increase in vascular disease, affecting both micro-vasculature (retinopathy, nephropathy, and neuropathy) and macro-vasculature (accelerated atherosclerosis, coronary and peripheral artery disease) that lead to accelerated cardiovascular disease.[21,22] Considering interventional outcomes, type 2 diabetes is an independent predictor of long-term mortality after coronary artery bypass grafting,[23] and diabetic patients undergoing percutaneous coronary intervention have an increased risk of intimal hyperplasia and restenosis compared with non-diabetic patients,[24,25] as well as decreased long-term survival.[26]

The hyperglycemic conditions in diabetes often coexist with dyslipidemia, inflammation, and extensive oxidative stress, which increases vascular wall stiffening due to crosslinking of the extracellular matrix (ECM).[27] Besides, the chronic tissue inflammation observed in diabetic patients is characterized by the increased presence of tissue resident macrophages with increased production of pro-inflammatory cytokines (e.g., TNF-α, IL-1β, IL-6, IL-8).[28–30]

It is to be expected that these diabetic conditions hamper the regenerative potential in patients, necessitating replacement vessels, and thus may impose difficulties when treating them with these resorbable synthetic vascular scaffolds. This is illustrated in a series of preclinical studies by the group of Deling Kong. In their first study, they report on improved remodeling and regeneration of arginine-glycine-aspartic acid (RGD)-functionalized vascular polycaprolactone (PCL) grafts compared with non-functionalized grafts in healthy rabbits.[31] In a second study, the same functionalized grafts were implanted in diabetic and non-diabetic rats.[32] The results showed that the promising effects of the RGD functionalization recorded in the healthy rabbits were not identified in the diabetic rats.

Only a few other studies have pre-clinically tested tissue engineered vascular grafts (e.g., subcutaneously implanted decellularized elastin scaffolds[33]) or implants (subcutaneous polyether-polyurethane sponge disks[34]) in both diabetic and non-diabetic animals. Although the heterogenous study setups and results hamper a fair comparison, a generic observation refers to a delayed inflammatory response around the implant, increased infectious complications, and a higher M1/M2 ratio in the diabetic versus non-diabetic animal models.[19]

Several *in vitro* studies aimed at shedding light on the effect of hyperglycemia on macrophages. These studies are, however, very heterogenous in their design (primary cells[35–38] or cell lines[39,40]) and interpretation of their results; thus, the direct effect of hyperglycemia is still a topic of debate.[19] Nevertheless, evidence suggests that monocytes/macrophages in *in vitro* hyperglycemic conditions adopt a more pro-inflammatory phenotype. In addition, it seems that macrophages fail to make the switch from pro-inflammatory M1-like to a pro-regenerative M2-like phenotype under hyperglycemic conditions, partly explaining the impaired wound healing in diabetic patients.[41,42] So far, the effect of normoglycemic versus hyperglycemic and hyperosmotic conditions on macrophages in three-dimensional (3D) synthetic scaffolds has not been investigated.

To gain a more fundamental understanding of the underlying cellular processes of macrophage-driven vascular tissue

regeneration in hyperglycemic conditions, the aim of this study was to investigate the human macrophage response in hyperglycemic conditions in terms of their inflammatory profile and ability to modulate tissue regeneration via a bottom-up *in vitro* approach. In the first set of experiments, primary human macrophages were seeded in two-dimensional (2D) gelatin-coated polystyrene well plates and exposed to normoglycemic (5.5 mM glucose), hyperglycemic (25 mM glucose), and osmotic control (OC) conditions (5.5 mM glucose, 19.5 mM mannitol). In the second set of experiments, macrophages were seeded in 3D electrospun resorbable PCL bisurea (PCL-BU) scaffolds, a supramolecular elastomer used in recent successful *in situ* tissue engineering applications. In the third set of experiments, macrophages were co-cultured with (myo)fibroblasts on PCL-BU scaffolds, to evaluate to what extent hyperglycemia affects macrophage-driven (myo)fibroblast activation.

Experiment

Detailed materials and methods are provided in the Supplementary Data—Supplementary Material and Methods S1.

Experimental outline

A stepwise approach was used to experimentally explore the effect of glycemic and osmotic conditions on macrophage polarization, and the interaction between macrophages, tissue-producing cells, and the scaffold (Fig. 1). Primary human peripheral blood-derived monocytes were differentiated into macrophages and polarized in 2D using cytokine stimulation in normoglycemic (5.5 mM glucose), hyperglycemic (25 mM glucose), and OC (5.5 mM glucose, 19.5 mM mannitol) medium in static culture conditions.

Cells and supernatant were analyzed using flow cytometry, quantitative polymerase chain reaction (qPCR), immunofluorescence (IF), and enzyme-linked immunosorbent assay (ELISA). Mono- and co-cultures of human macrophages and (myo)fibroblasts (human saphenous venous cells) in 3D electrospun PCL-BU scaffold were evaluated using qPCR, IF, ELISA, and biochemical assays to determine hydroxyproline (HYP), glycosaminoglycan (GAG), and DNA content.

Normoglycemic, hyperglycemic, and OC medium

For the monocyte/macrophage cultures and experiments, medium consisted of SILAC RPMI (Roswell Park Memorial Institute) 1640 Flex Media (no glucose, no phenol red; Gibco), supplemented with 2% pooled human serum (Sanquin Blood Bank; the optimal human serum concentration was previously validated in our lab for buffy coat derived macrophages[43]), 1% penicillin-streptomycin (Pen-Strep), 1% 100 mM sodium pyruvate, 1% N-(2-hydroxyethyl)piperazine-N′-(2-ethanesulfonic acid), 4-(2-hydroxyethyl)piperazine-1-ethanesulfonic acid (HEPES) 1M buffer solution, 1% glutamax (all from Gibco). Then, 5.5 mM glucose solution (Gibco) was added for normoglycemic medium, 25 mM glucose solution for hyperglycemic medium, and 5.5 mM glucose with 19.5 mM mannitol (Fluka) was added for the OC.[44]

For the (myo)fibroblast cultures and experiments, the normoglycemic medium consisted of Dulbecco's modified Eagle medium (DMEM; low glucose, 1 g/L [5.55 mM glucose]; Gibco), supplemented with 1% Pen-Strep, 1% minimal Essential Medium (MEM) non-essential amino acids (NEAA; Gibco), and 2% human serum. For OC medium, DMEM low-glucose medium was supplemented with 19.5 mM mannitol, 1% Pen-Strep, 1% MEM NEAA, and 2% human serum. The hyperglycemic (myo)fibroblast medium consisted of Advanced DMEM (high glucose, 4.5 g/L [25 mM glucose]; Gibco), supplemented with 2% human serum, 1% Pen-Strep, and 1% glutamax.

For the 3D co-culture experiments of monocytes/macrophages and (myo)fibroblasts, corresponding glycemic and osmotic RPMI and DMEM medium with 0.25 mg/mL L-ascorbic acid 2-phosphate (Sigma) were mixed in a 1:1 (v/v) ratio and added to the constructs.

Cell isolation and culture

Human peripheral blood mononuclear cells (hPBMCs) were isolated from buffy coats of healthy donors (Supplementary Table S1) from Sanquin Blood Bank (Sanquin, The

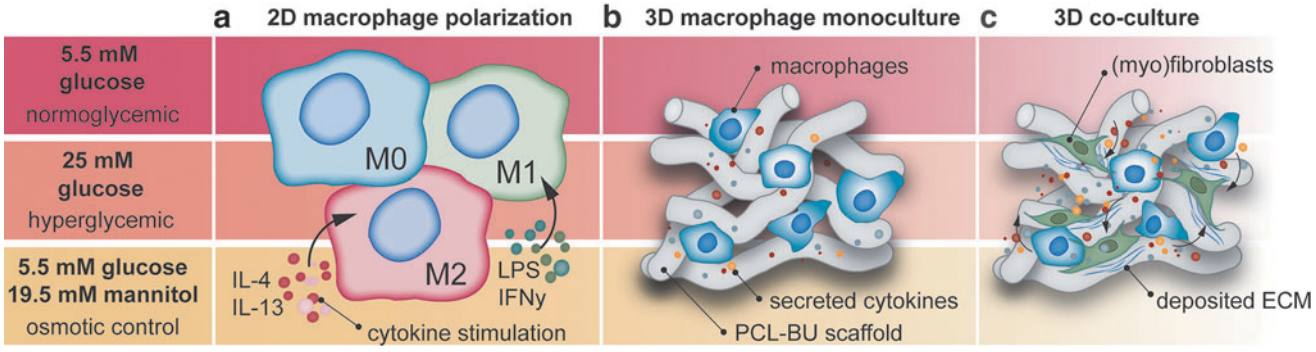

FIG. 1. Experimental set-up depicting the bottom-up approach of the study, with all 2D and 3D experiments performed in normoglycemic (5.5 mM glucose), hyperglycemic (25 mM glucose), and the OC (5.5 mM glucose, 19.5 mM mannitol); **(a)** monocyte-derived macrophage polarization toward M1 (with LPS, IFN-γ) and M2 (with IL-4, IL-13) phenotype; **(b)** monoculture of macrophages on PCL-BU scaffold, and **(c)** co-cultures of cytokine-secreting macrophages and ECM-depositing (myo)fibroblasts. *Black arrows* depict the directing role of the macrophage in tissue deposition by the fibroblast via direct and paracrine crosstalk. 2D, two-dimensional; 3D, three-dimensional; ECM, extracellular matrix; IFN-γ, interferon-γ; IL, interleukin; LPS, lipopolysaccharide; OC, osmotic control; PCL-BU, bis-urea-modified polycaprolactone.

Netherlands) using density gradient centrifugation on isoosmotic medium. The buffy coats were obtained from anonymized volunteers that provided written informed consent, as approved by the Sanquin Research Institutional Medical Ethical Committee. After all isolation steps were performed, the PBMCs were placed in a cell culture flask to allow for the adherence of monocytes. After 1 h, nonadherent cells were washed away with phosphate-buffered saline and the remaining monocytes were used for further macrophage differentiation.

(Myo)fibroblasts were isolated from leftover saphenous vein samples from one donor (female, 62 years) after coronary by-pass surgery by previously established protocols,[45] in accordance with the Dutch advice for secondary-use material.

Macrophage differentiation and polarization

Monocyte/macrophage medium with the selected glucose concentration or osmotic pressure was supplemented with 20 ng/mL macrophage colony-stimulating factor (M-CSF, PeproTech) and added to the adherent cells to initiate macrophage differentiation. After 5 days of M-CSF stimulation, the cells were detached with accutase (STEMCELL) and seeded in well plates (seeding density 1.5×10^5 cells/cm^2). For the 2D experiments, the monocyte-derived macrophages were polarized toward different polarization states using previously described cytokines.[46] For M1 macrophages, 100 ng/mL lipopolysaccharide (LPS; Sigma Aldrich) and 100 ng/mL interferon γ (IFN-γ) was added, and 40 ng/mL interleukin (IL)-4 and 20 ng/mL IL-13 (all PeproTech) for M2 macrophages. No additional cytokines were added for the M0 macrophages. The macrophages were polarized for 2 subsequent days.

Scaffold preparation and sterilization

Electrospun scaffold sheets ($\sim10\times10$ cm^2) were produced from polymer solutions containing 15% (w/w) bis-urea-modified PCL (PCL-BU, SyMO-Chem) and 85% (w/w) of chloroform/methanol ($CHCl_3$/MeOH, 98:2; $CHCl_3$, Sigma; MeOH, VWR Chemicals), which was stirred overnight at room temperature. The polymer solutions were electrospun in a climate-controlled chamber (23°C and 30% humidity; IME Technologies) using a flow rate of 40 μL/min, an applied voltage of 16 kV on the electrospinning nozzle, −1 kV on a rotating cylindrical target, and a constant distance between nozzle and target of 16 cm. The obtained scaffold was dried under vacuum overnight, to remove solvent remnants. The scaffold was cut into Ø8 mm circles using a biopsy punch (KAI Medical) before sterilizing by ultraviolet (UV) light. Subsequently, the scaffold was placed in membrane-free cell culture inserts (6.5 mm; Corning) using a custom-made UV-sterilized polyether ether ketone ring.

Cell seeding in scaffold

For the 3D experiments, cells were seeded in electrospun PCL-BU scaffold, using fibrin as a cell carrier, as previously developed,[47] and as extensively described elsewhere.[48] Cells (monocultures: 30×10^6 macrophages/cm^3 or 15×10^6 [myo]fibroblasts/cm^3; co-culture: 30×10^6 macrophages/cm^3 and 15×10^6 [myo]fibroblasts/cm^3) were resuspended in 15 μL of bovine thrombin (10 IU/mL) in medium and mixed with fibrinogen solution (10 mg/mL; both Sigma) at double the volume of thrombin and cells. The mixture was dripped onto the scaffold and allowed to polymerize for 30 min. Subsequently, the wells were filled with 1.5 mL medium. The experiment was ended after 7 days, and samples were stored for analysis.

Analysis

The collected supernatant was processed, and the secretion of a set of proteins related to macrophage polarization (Supplementary Table S2) was quantified at the Multiplex core facility of the Laboratory for Translational Immunology of the University Medical Centre Utrecht, the Netherlands, using a multiplex immunoassay based on Luminex xMAP technology (Luminex). From the measured cytokines, a simplified M1/M2 ratio was calculated by classifying the cytokines as primarily M1- or M2-associated, as also previously described[49,50] (details in Supplementary Data).

Phenotypic analysis of 2D cultured macrophages was performed using flow cytometry, with the following antibodies: FITC-conjugated anti-human CD80 (M1 cell surface marker), PE/Cy5-conjugated anti-human CD206 (M2 cell surface marker), and APC-conjugated anti-human CD163 (M2 cell surface marker) and Zombie NIR™ were used as a viability dye (all from BioLegend). All samples were analyzed using a FACSAria (BD Biosciences), and data were analyzed using FlowJo Software (version 10, BD Life Sciences).

Samples from 2D experiments were collected, lysed using RNeasy Mini Kit lysis buffer (Qiagen), and stored at −30°C. Samples from 3D experiments were first disrupted using a micro-dismembrator (Sartorius), as described earlier.[49] Total RNA was isolated using the Qiagen RNeasy kit following supplier instructions. After isolation, RNA quantity and purity were analyzed with a spectrophotometer (NanoDrop, ND-1000, Isogen Life Science). cDNA was synthesized in a thermal cycler (C1000 Touch, Bio-Rad); it was specifically amplified by PCR using human-specific primers to detect mRNA levels of a selection of genes encoding for macrophage polarization, ECM constituents, and ECM remodeling markers (for list and primer sequences, see Supplementary Table S3).

Samples of 2D experiments were fixed and stained for morphology assessment with phalloidin-atto 488 and 4′,6-diamidino-2-phenylindole (DAPI), for (pro-)collagen with CNA35-OG488 and DAPI.[51] The coverslips were placed on microscopy slides using Mowiol (Sigma-Aldrich), and they were visualized using an inverted epifluorescence microscope (Zeiss Axiovert 200 M, with a 40×/0.95NA Plan-Apochromat lens). For localization of monocyte-derived macrophages and (myo)fibroblasts in the 3D co-culture constructs, a whole-mount staining was performed with markers CD45 and vimentin (VIM), respectively, and DAPI (Supplementary Table S4). Scaffold samples were washed again and stored in Mowiol until imaging with a confocal laser scanning microscope (Leica TCS SP5X, with a 63×1.1 HCX-PL ApoCS Lens).

Mono- and co-culture samples stored for biochemical assay analysis were lyophilized overnight, weighed, reduced to a powder with the micro-dismembrator, and digested

before determining the HYP, GAG, and DNA content as described earlier.[49]

Statistical analysis

Detailed information on sample size (n) and donor are given in the results section and figure legends. Data are expressed as individual data points in scatter plots with a grand mean. Statistical analysis was performed with GraphPad Prism 8.0. When data were normally distributed, statistical significance was tested using one-way analysis of variance with a Tukey's multiple-comparison test. When data were not normally distributed, the non-parametric Kruskal–Wallis test with a Dunn's multiple-comparison test were performed to test statistical significance. Differences were considered significant for $p < 0.05$ and visualized with $*p < 0.05$ or $**p < 0.01$.

Experimental Results

Glucose concentration and osmotic pressure do not affect macrophage cell morphology and polarization effectiveness

Immunofluorescent staining of F-actin cytoskeleton was performed to gain insight in the effectiveness of polarization on a morphological level (Fig. 2). The M1 polarized macrophages typically presented with a more rounded ''fried-egg''-like morphology, whereas the M2 polarized macrophages displayed a more elongated, spindle-like morphology in all three glycemic and osmotic conditions. In the unpolarized M0 group, a combination of rounded and more elongated cells was observed in all different media conditions for all donors ($n = 3$).

On gene expression (Supplementary Fig. S1a) and cell surface marker (Supplementary Fig. S1b) expression levels, the cytokine-induced macrophage polarization was shown to be effective, regardless of glucose concentration or donor. Finally, the metabolic marker expression *SCL2A1* encoding for glucose transporter 1 was upregulated in the M1 polarized group when compared with the non-polarized and M2 polarized macrophages, in all glycemic conditions for all three donors (Supplementary Fig. S2).

In contrast, the fatty acid transporter *CD36* was less expressed in M1 polarized macrophages compared with M0 and M2 groups, again for all glycemic conditions for all three donors. Overall, biochemically induced macrophage polarization was robustly retained in all glycemic and osmotic conditions for all donors tested.

Hyperosmotic pressure, and not solely hyperglycemia, enhances cytokine gene expression responses in polarized macrophages

Having established that macrophage polarization is largely unaffected by the different glycemic and osmotic conditions, we assessed the effect of hyperglycemia for each

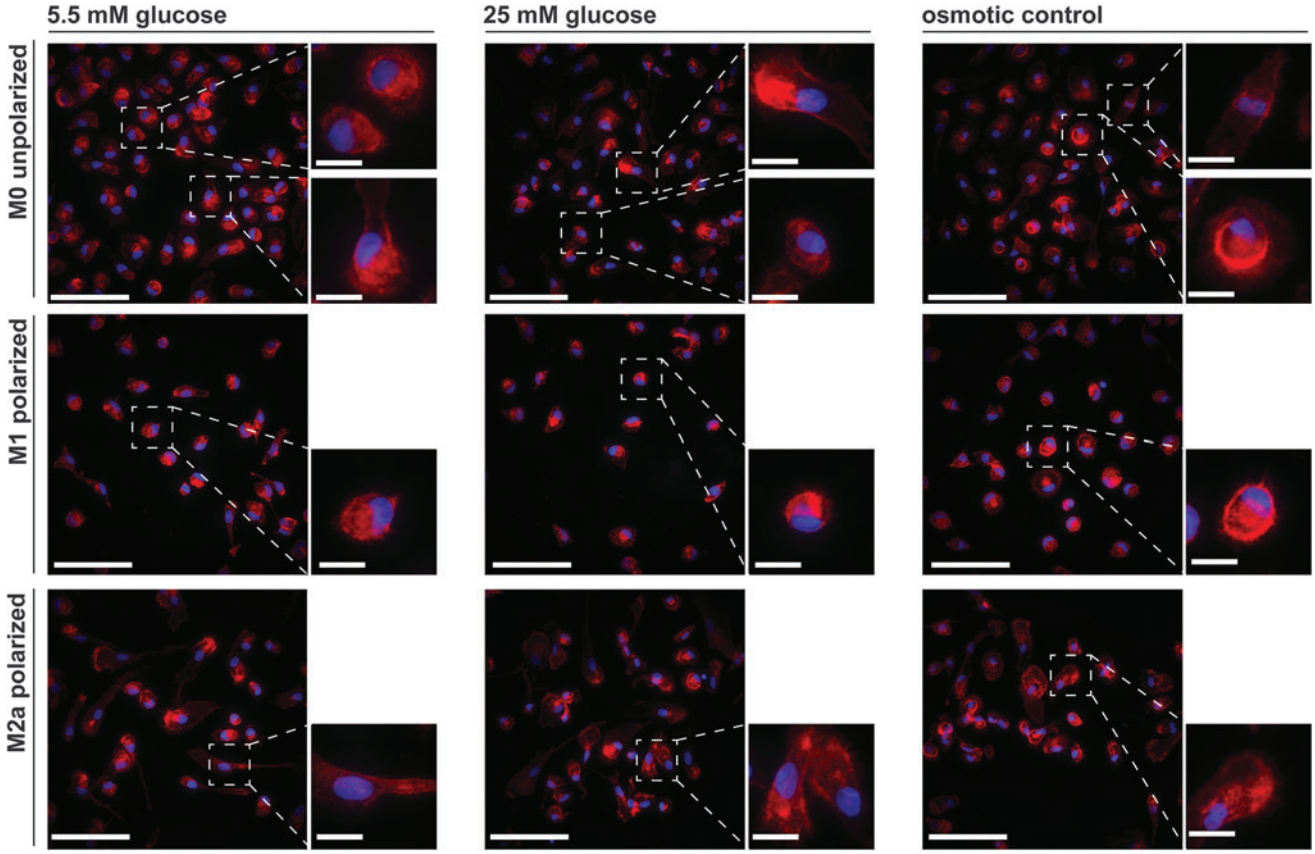

FIG. 2. Morphological patterns of polarized macrophages in 2D in normoglycemic, hyperglycemic, and OC. Immunofluorescent staining of F-actin cytoskeleton (*red*) and cell nuclei (*blue*) illustrating changes in cellular morphology after polarization into different phenotypes, with more rounded M1-like and the elongated M2-like morphology. Scalebar overview images 50 μm, zooms 20 μm.

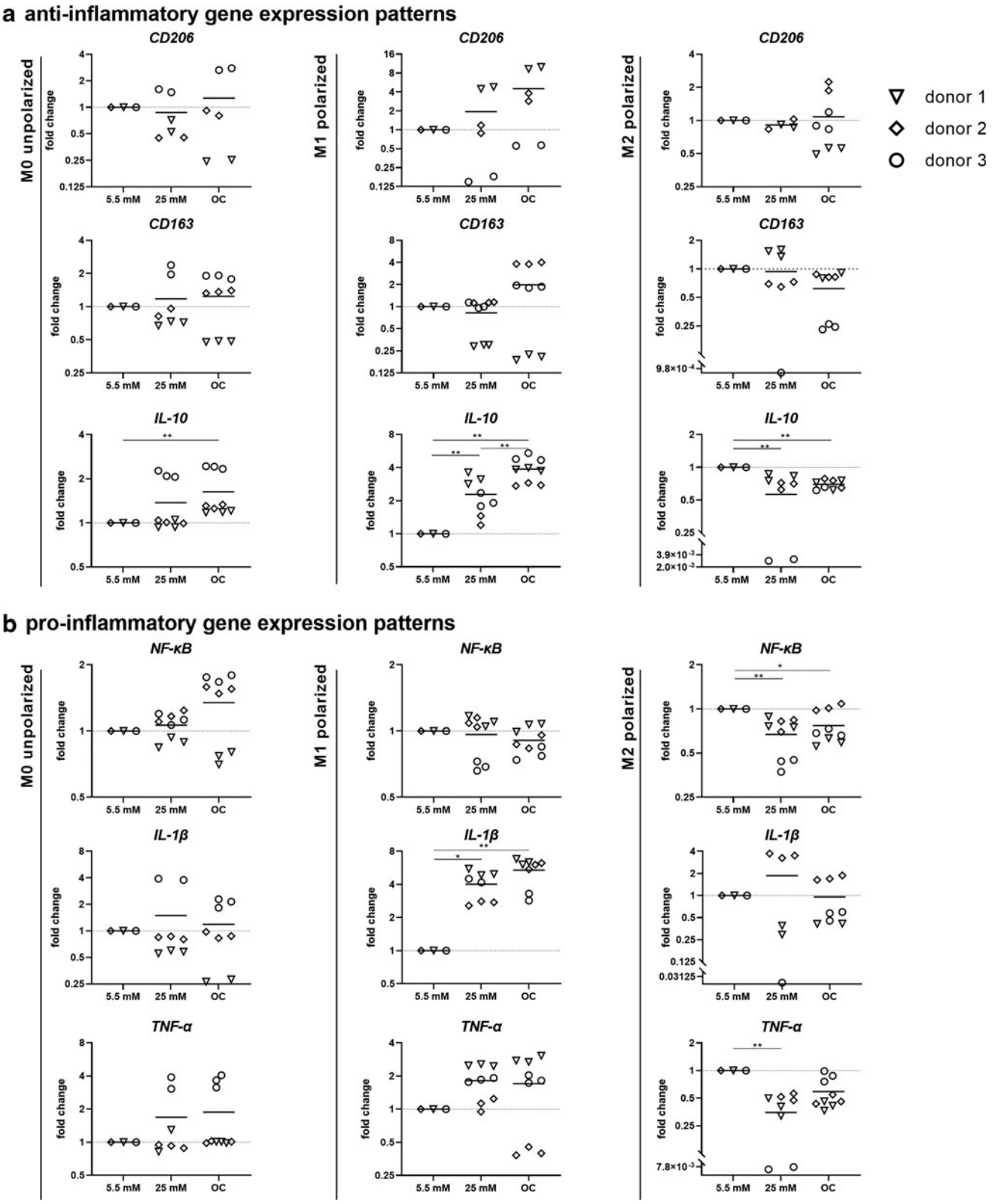

FIG. 3. Gene expression patterns of differently polarized monocytes/macrophages (M0, M1, M2) in 2D in hyperglycemic and OC compared with the normoglycemic group. **(a)** Fold change of anti-inflammatory associated genes (*CD206, CD163, IL-10*) and **(b)** pro-inflammatory associated genes (*NF-kB, IL-1β, TNF-α*). Significant differences presented as: $*p < 0.05$, $**p < 0.01$. CD, cluster of differentiation; NF-κB, nuclear factor kappa-light-chain-enhancer of activated B cells; TNFα, tumor necrosis factor α.

individual polarization state (Fig. 3a). Gene expression analysis of anti- and pro-inflammatory genes of the unpolarized and polarized macrophages in different glycemic and osmotic conditions showed substantial donor-to-donor variation. Nevertheless, in M1 polarized macrophages, *IL-10* gene expression was significantly increased in both the hyperglycemic and OC, indicating that the effect is due to the change in osmotic pressure, rather than the high glucose alone. Similarly, the M1 macrophages showed increased *IL-1β* gene expression under both hyperglycemic and hyperosmotic conditions (Fig. 3b). Similar, yet non-significant trends were observed for *CD206* and *TNF-α* expression.

For M2 macrophages, a significant drop in anti-inflammatory *IL-10* and pro-inflammatory *NF-kB* gene expression was observed for both hyperglycemic and hyperosmotic conditions, as well as for *TNF-α* expression. This again indicates that the observed effect on macrophage cytokine gene expression patterns is not solely due to higher glucose levels, but it is predominantly governed by hyperosmotic stress.

Further, cytokine secretion profiles were measured in the supernatant ($n=3$ donors) (Fig. 4a). Unpolarized M0 macrophages in normo- and hyperglycemic conditions showed the highest secretion of macrophage-derived chemokine (MDC) compared with the OC. However, vascular endothelial growth factor (VEGF) secretion in M0 macrophages tended to increase in hyperglycemic conditions. Relatively similar patterns were observed in cytokine excretion of M2 polarized macrophages. M1 polarized macrophage cytokine secretion, on the other hand, showed different patterns, with higher TNF-α and latency-associated protein (LAP) in the normoglycemic control compared with the OC.

Secretion of other proteins was similar in all glycemic and osmotic conditions for the M1 polarized macrophages. The M1/M2 ratios that were determined based on the secretion levels of pro- and anti-inflammatory cytokines demonstrate that the polarization to M1 macrophages was effective in all three glycemic conditions (Fig. 4b).

SCL2A1 and CD36 gene expression patterns tend to show increased expression in hyperglycemic and hyperosmotic conditions

When normalizing gene expression patterns of the metabolic markers *SCL2A1* and *CD36* to the normoglycemic conditions, an overall trend of increased expression for both *SCL2A1* and *CD36* was observed in both hyperglycemic and hyperosmotic conditions (Fig. 5). This was observed for all different macrophage polarization states and donors, except for *CD36* gene expression in M2 polarized macrophages, in which only the high glucose conditions, and not the OC, led to an almost three-fold increase in *CD36* expression. In addition, *SCL2A1* expression in unpolarized M0 and M1 polarized macrophages showed some inter-donor variation, with unaltered or decreased gene expression of *SCL2A1* in hyperglycemic and hyperosmotic conditions compared with normoglycemia for donor 1, in contrast to donors 2 and 3.

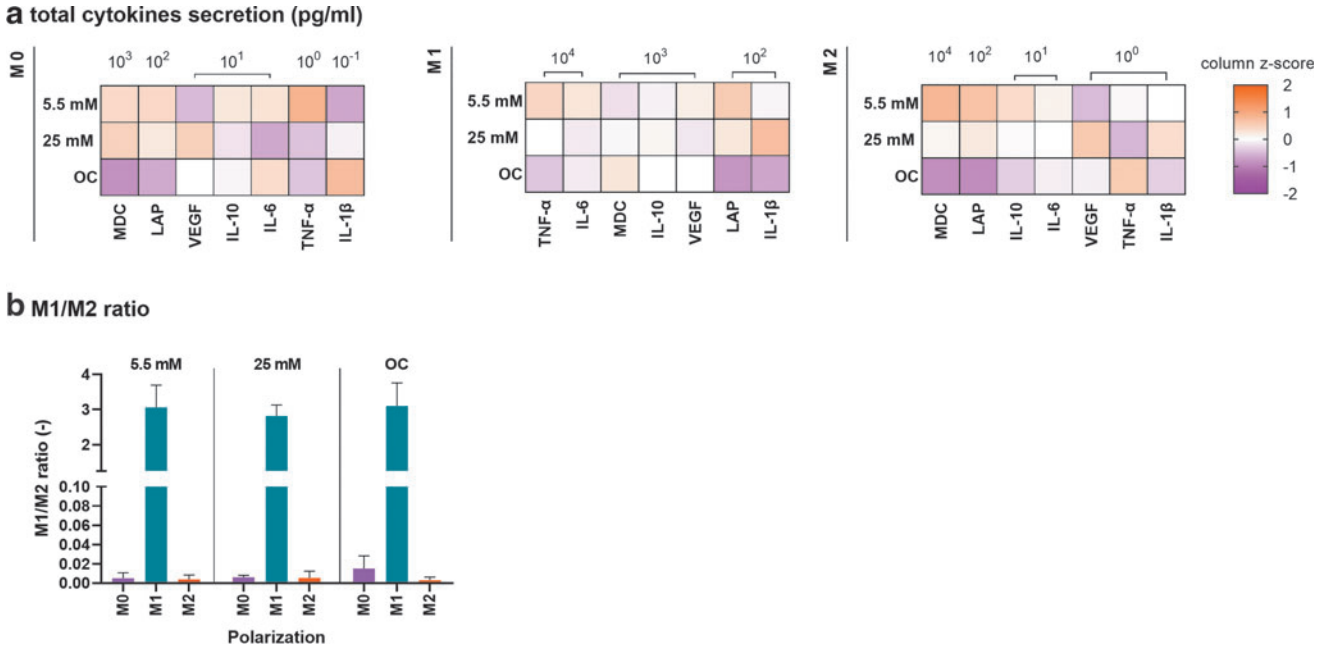

FIG. 4. Total cytokine secretion of differently polarized monocytes/macrophages (M0, M1, M2). **(a)** total cytokine secretion measured via ELISA. qPCR data ($n=3$) are plotted as fold change (compared with 5 mM glucose group); **(b)** M1/M2 ratios based on the cytokine secretion levels of IL1β, IL6, TNF-α (pro-inflammatory) and LAP, MDC (anti-inflammatory). ELISA data ($n=3$) are transformed into z-score (i.e., number of standard deviations from the mean value), showing increased (*orange*) or decreased (*purple*) or average (*white*) expression levels of the protein of interest. Vertical columns representing the protein of interest are ordered from highest (*right*) to lowest (*left*) absolute quantities measured in the supernatant. ELISA, enzyme-linked immunosorbent assay; LAP, latency-associated protein; MDC, macrophage-derived chemokine; qPCR, quantitative polymerase chain reaction.

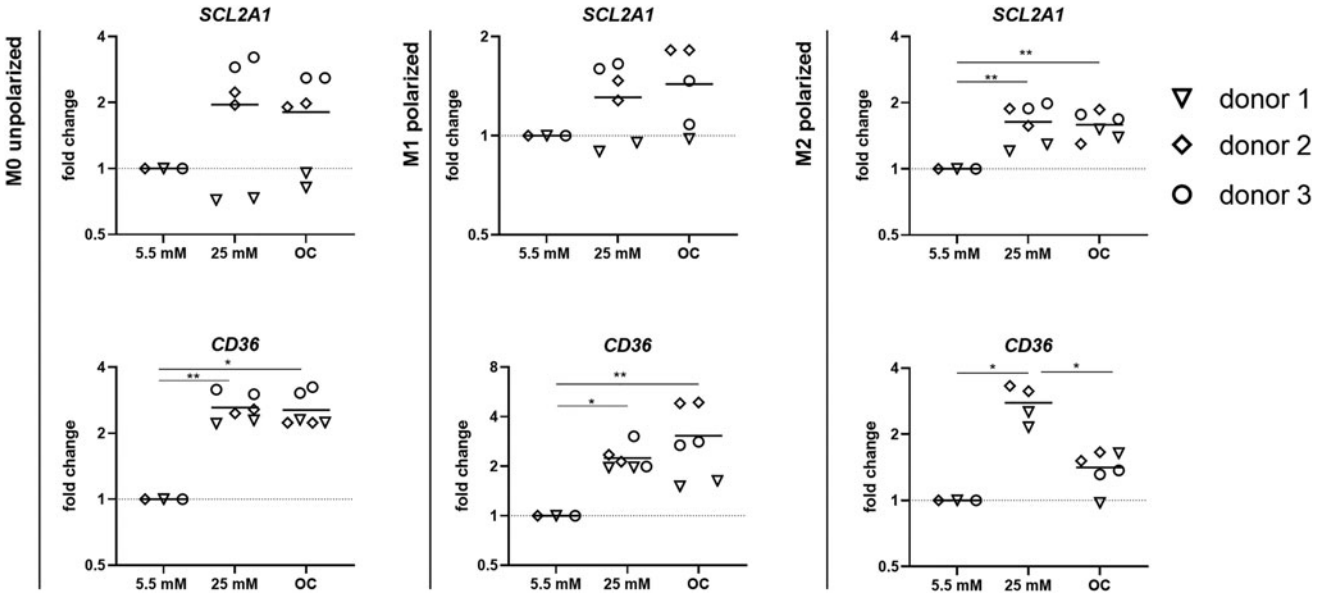

FIG. 5. *SCL2A1* and *CD36* gene expression on polarized macrophages in hyperglycemic and OC compared with the normoglycemic group. qPCR data ($n=3$) are plotted as fold changes in relative expression of *SCL2A1* encoding for glucose transporter 1 and *CD36* encoding for scavenger receptor fatty acid transporter. Significant differences are presented as: $*p<0.05$, $**p<0.01$.

Scaffold-induced polarization of monocyte-derived macrophages in hyperosmotic conditions results in a mixed macrophage phenotype

To probe the influence of hyperglycemia on the macrophage response to a biomaterial, monocyte-derived macrophages ($n=4$ donors) were seeded on degradable electrospun scaffold and cultured for 7 days. The scaffold was 134.4 ± 11 μm thick, and it had an isotropic fiber distribution and a fiber diameter of 3.4 ± 0.5 μm (Supplementary Fig. S3). After 7 days, monocyte-derived macrophage presence and homogeneous distribution was confirmed in all glycemic and osmotic conditions with CD45 staining (Supplementary Fig. S4). In contrast to the chemical polarization in the 2D experiments, scaffold-induced polarization of the monocyte derived macrophages resulted in a less clear distinctive macrophage phenotype (Supplementary Fig. S5a).

Besides, a relatively large donor heterogeneity was observed (Fig. 6a), with donor 6, in particular, showing opposite responses to high glucose conditions when compared with the other donors. Nevertheless, a significant increase in pro-inflammatory *TNF-α* gene expression was observed in hyperosmotic conditions when compared with normoglycemic conditions, paired with a trend in increased anti-inflammatory *CD206* gene expression. Anti-inflammatory marker *CD163*, often used to identify the M2 macrophage phenotype, showed an unexpected effect of only an increased expression in the OC, compared with the normoglycemic and hyperglycemic group. *IL-10*, an anti-inflammatory cytokine known for its inhibitory effects on collagen production, showed a very large donor variation on gene expression level, and thus no clear effect of glycemic or osmotic conditions.

This is also reflected in the total cytokine secretion in the supernatant (Fig. 6b). Of the selection of cytokines that was measured in the supernatant with ELISA, MDC, a cytokine involved in monocyte/macrophage migration and infiltration, was measured in highest concentrations, followed by pro-inflammatory IL-6, anti-inflammatory LAP, and regulator of angiogenesis VEGF. Compared with the cytokine secretion patterns in the chemically polarized macrophages in 2D (Fig. 4), the scaffold-induced polarization of macrophages led to a mixed macrophage phenotype, with relatively high levels of MDC and LAP (similar to the 2D M2 polarized macrophages), as well as relatively high levels of IL-6 and VEGF (similar to the M1 polarized macrophages). The M1/M2 ratios showed that the macrophage cultures in hyperglycemia had a slightly higher pro-inflammatory cytokine secretion (Fig. 6c).

Metabolic markers *SCL2A1* and *CD36* expressed by the macrophages seeded on the scaffold showed a clear response to glycemic and osmotic stimuli (Fig. 6d). Although some donor heterogeneity was observed, with again donor 6 responding differently compared with the other donors, hyperglycemia led to reduced *SCL2A1* gene expression, while increasing *CD36* expression, with the latter effect being particularly strong in the hyperosmotic group (Fig. 6d).

Gene expression of ECM remodeling markers *MMPs* and *TIMPs* in the macrophage monoculture showed a relatively large donor heterogeneity, with again donor 6 showing opposite patterns compared with the other donors (Supplementary Fig. S6). Only in *MMP1* and *TIMP1* expression, a minor trend toward increased expression was observed in the hyperglycemia group, however not significant, due to the large inter-donor variation.

Co-culture of monocyte-derived macrophages and (myo)fibroblasts on scaffold in hyperglycemic conditions tends to result in a more pro-inflammatory environment with increased collagen gene expression levels

To evaluate to what extent hyperglycemia affects macrophage-driven (myo)fibroblast activation, macrophages

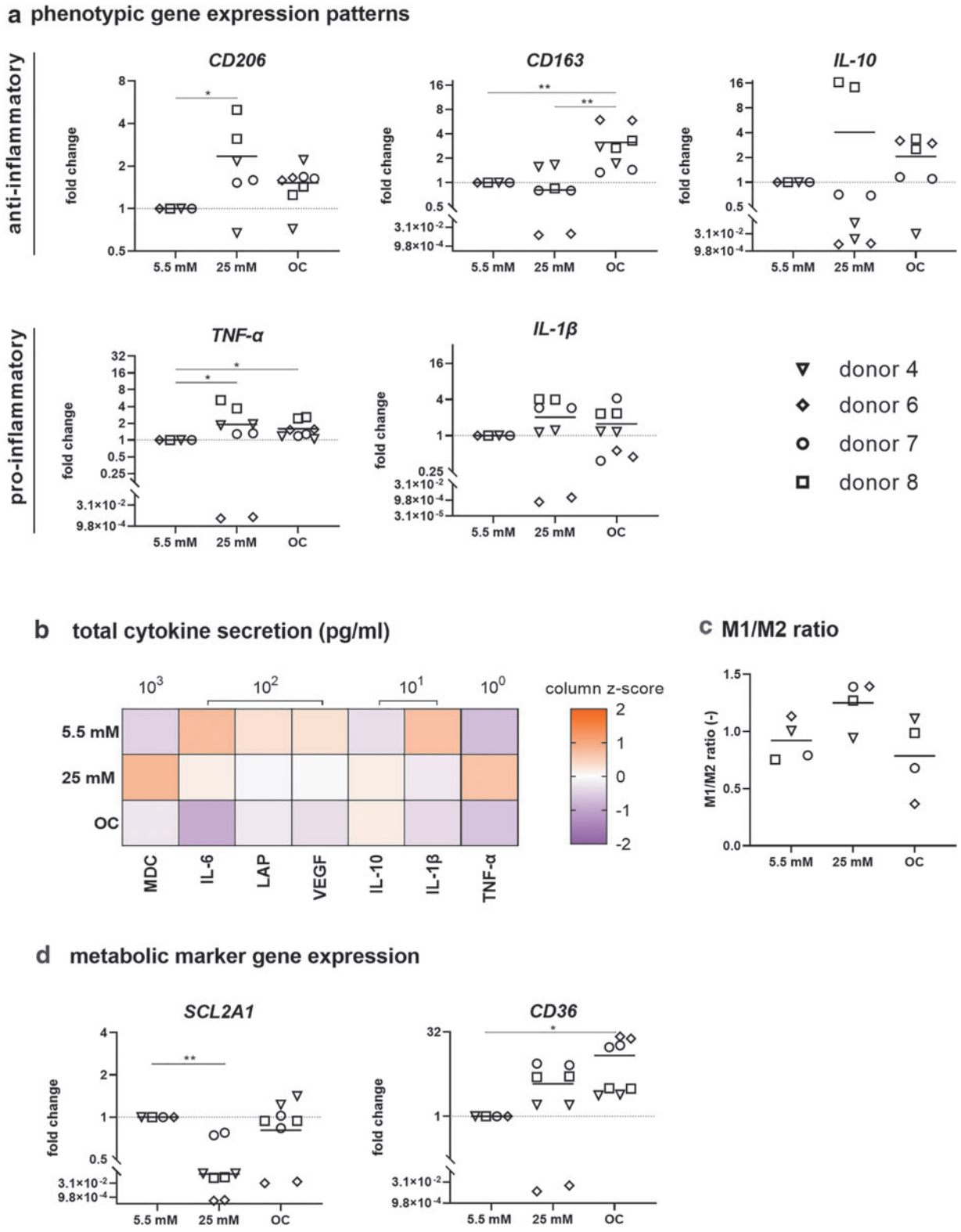

FIG. 6. Phenotypic gene expression patterns, total cytokine secretion, and metabolic marker gene expression of monocytes/macrophages cultured in 3D PCL-BU scaffold in hyperglycemic and OC compared with the normoglycemic group. Fold changes of relative expression of **(a)** anti-inflammatory associated genes (*CD206, CD163, IL-10*) and pro-inflammatory associated genes (*TNF-α, IL-1β*); **(b)** heat map of total cytokine secretion; **(c)** M1/M2 ratios based on the cytokine secretion levels of IL-1β, IL-6, TNF-α (pro-inflammatory) and LAP, MDC (anti-inflammatory); **(d)** Fold change metabolic markers *SCL2A1* encoding for glucose transporter 1 and *CD36* encoding for scavenger receptor fatty acid transporter. qPCR data ($n = 4$) are plotted as fold change (compared with the 5 mM glucose group). Significant differences presented as: $*p < 0.05$, $**p < 0.01$. ELISA data ($n = 4$) are transformed into z-score (i.e., number of standard deviations from the mean value), showing increased (*orange*) or decreased (*purple*) or average (*white*) expression levels of the protein of interest. Vertical columns representing the protein of interest are ordered from highest (*right*) to lowest (*left*) absolute quantities measured in the supernatant. VEGF, vascular endothelial growth factor.

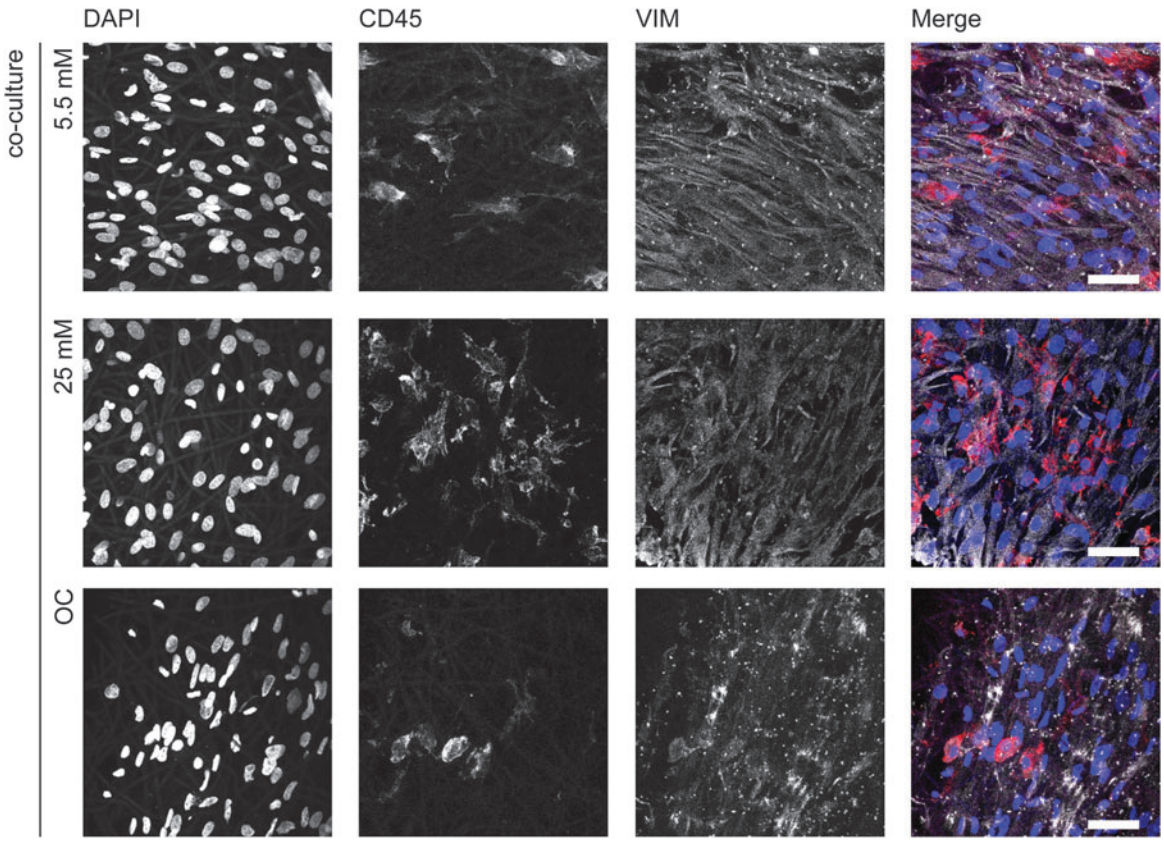

FIG. 7. Co-culture of monocyte-derived macrophages and (myo)fibroblasts (HVSCs) cultured on PCL-BU scaffold for 7 days in normoglycemic, hyperglycemic, and OC. Representative overlays of z-stack (±60 μm) images with monocyte marker CD45 (*red*), fibroblast marker VIM (*gray*), and cell nuclei (DAPI, *blue*) in grayscale and overlay. Scale bars 50 μm. DAPI, 4′,6-diamidino-2-phenylindole; HVSCs, human saphenous venous cells; VIM, vimentin.

were co-cultured with (myo)fibroblasts on PCL-BU scaffold. After 7 days of co-culture, both cell types were still present, as demonstrated by positive staining for both the monocyte marker CD45 and fibroblast marker VIM(Fig. 7). The macrophages demonstrated a predominantly rounded morphology.

Similar to the macrophage monoculture on scaffold, large donor heterogeneity was observed in the co-culture for the macrophage phenotypic gene expression markers (Fig. 8a), resulting in an overall mixed phenotypic image (Supplementary Fig. S5b).

IL-1β gene expression was significantly higher in the hyperglycemic group and showed a trend of increased expression in the OC group, compared with the normoglycemic group. However, IL-1β cytokine secretion showed a different pattern, in which the OC group showed the lowest expression compared with the normo-glycemic and hyperglycemic group (Fig. 8b). *ACTA2* expression, the gene coding for αSMA, showed higher expression in the hyperglycemic group, which was also observed in the (myo)fibroblast monoculture (Supplementary Fig. S7a).

The selection of cytokines measured in the supernatant depicted a micro-environment for the co-culture in which pro-inflammatory cytokines IL-6 and MDC were present in relatively high levels (Fig. 8b), similar to the chemically polarized M1 macrophages in 2D (Fig. 4a) and 3D macrophage monoculture (Fig. 6b). Hyperglycemia and hyperosmotic pressure led to an increased IL-6 secretion by the

FIG. 8. Gene expression patterns, biochemical assays, and total cytokine secretion of co-cultures of monocytes/macrophages and HVSCs cultured in 3D PCL-BU scaffold in hyperglycemic and OC compared with the normoglycemic group. Fold change of **(a)** phenotypic markers with both anti-inflammatory associated genes (*CD206, CD163, IL-10*) and pro-inflammatory associated genes (*TNF-a*, *IL-1β*) and fibroblast marker (*ACTA2*—αSMA); **(b)** heat map of total cytokine secretion; **(c)** M1/M2 ratios based on the cytokine secretion levels of IL1β, IL6, TNF-α (pro-inflammatory) and LAP, MDC (anti-inflammatory); **(d)** biochemical assays of 3D co-cultures; **(e)** ECM (*Col1A1*, *Col3A1*, *ELN*) and ECM remodeling markers (*MMPs* and *TIMPs*). qPCR data ($n=4$) are plotted as fold change (compared with 5 mM glucose group). Biochemical assay data ($n=4$) are corrected against dry weight and DNA. Significant differences presented as: $*p<0.05$, $**p<0.01$. ELISA data ($n=4$) are transformed into z-score (i.e., number of standard deviations from the mean value), showing increased (*orange*) or decreased (*purple*) or average (*white*) expression levels of the protein of interest. Vertical columns representing the protein of interest are ordered from highest (*right*) to lowest (left) absolute quantities measured in the supernatant. GLUT, glucose transporter; TIMP, metallopeptidase inhibitor; MMP, matrix metalloproteinase.

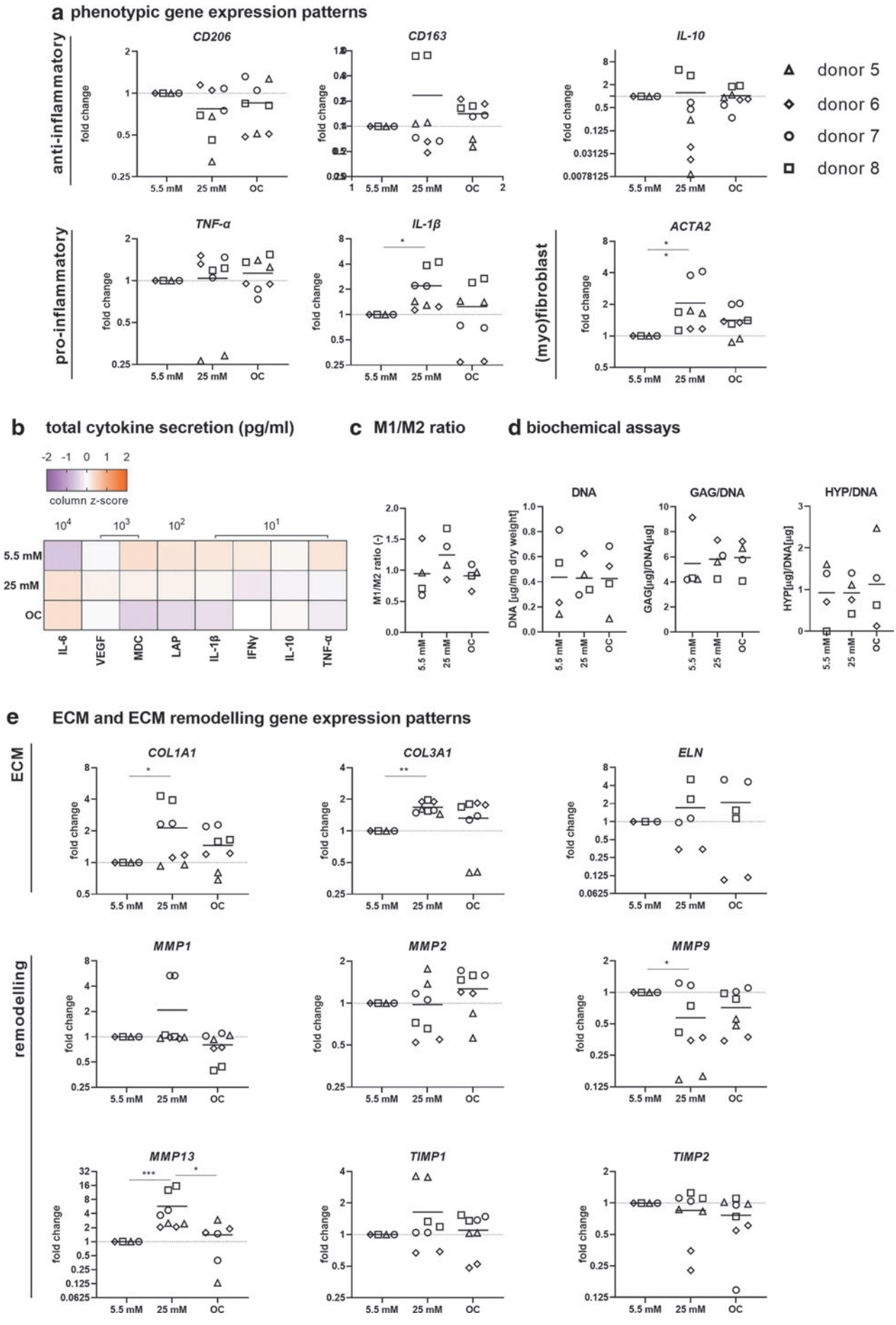

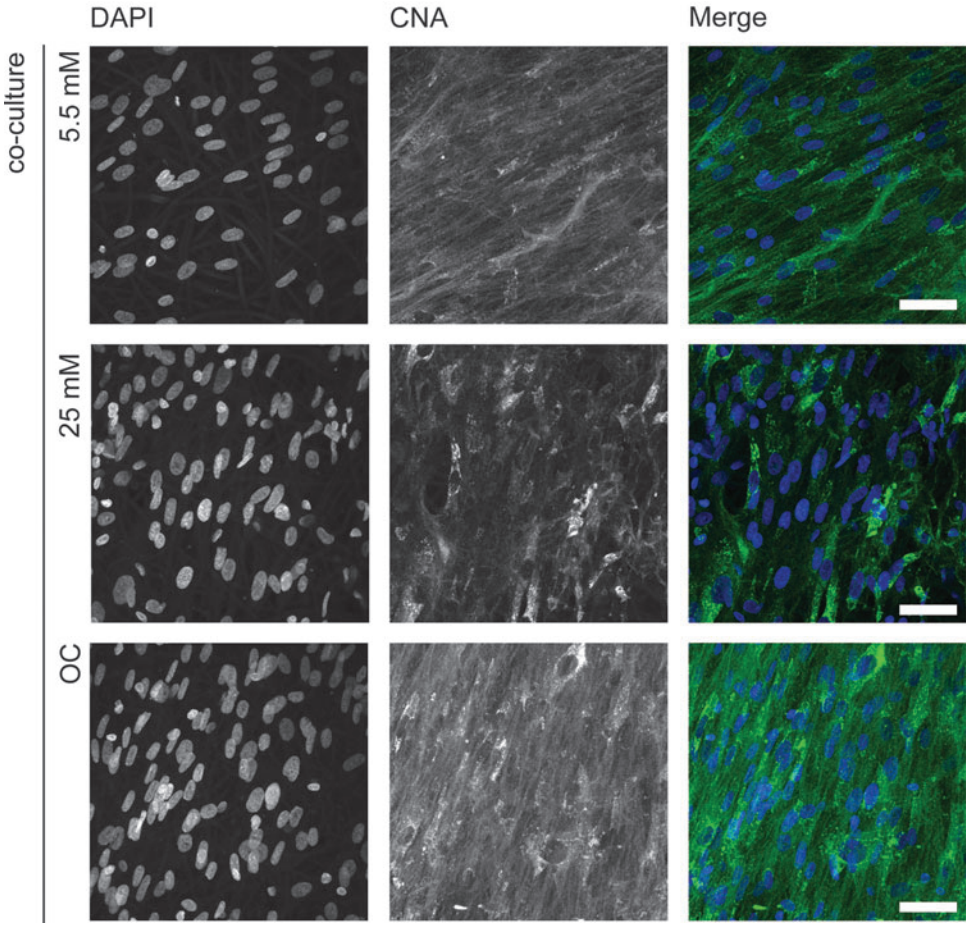

FIG. 9. Collagen production of co-culture of monocyte-derived macrophages and (myo)fibroblasts (HVSCs) cultured on PCL-BU scaffold for 7 days in normoglycemic, hyperglycemic, and OC. Representative overlays of z-stack (±60 μm) images with CNA35-OG488 probe, and cell nuclei (DAPI, *blue*) in grayscale and overlay. Scale bars 50 μm.

cells in co-culture (Fig. 8b). The (myo)fibroblasts were most probably important contributors to the overall IL-6 and VEGF cytokine secretion in the co-culture, as the IL-6 and VEGF levels were comparable to the secretion levels in the (myo)fibroblast monoculture (Supplementary Fig. S7d), whereas IL-6 and VEGF cytokine secretion levels in the macrophage monoculture were slightly lower (Fig. 6b).

The M1/M2 ratios showed minor differences between the glycemic and osmotic conditions, although the co-cultures in hyperglycemia showed a small trend toward more pro-inflammatory secretion (Fig. 8c).

In terms of tissue production, no clear effect of hyperglycemia or osmotic pressure was seen at the protein level. Biochemical assays showed that the cells did produce GAG and HYP in all conditions (Fig. 8d). Collagen production was further confirmed by CNA staining (Fig. 9).

When comparing tissue levels of the co-culture with the (myo)fibroblast monoculture, it was observed that the (myo)fibroblast monoculture resulted in substantial higher GAG and HYP levels (Supplementary Fig. S7c), suggesting an inhibitory effect of the macrophages. However, no clear differences between the glycemic or osmotic groups were observed in terms of GAG and HYP measurements after 7 days of culture. On the contrary, at a gene expression level, hyperglycemic conditions demonstrated to increase collagen expression and *MMP13*, and decrease *MMP9* expression (Fig. 8e), suggesting a differently regulated collagen remodeling.

Again, when comparing the collagens gene expression (*COL1A1* and *COL3A1*) of the co-culture with the (myo)fibroblast monoculture (Supplementary Fig. 7b), the (myo)fibroblasts contributed to a large extent to the observed effect of increased expression in response to hyperglycemia. Of note, in the (myo)fibroblast monoculture, the increased expression (trends) of *ACTA2* and ECM gene expression markers were merely an effect of high glucose and not hyperosmotic pressure (which we did observe in general in the macrophage cultures). Finally, the metabolic marker expression *SCL2A1* and *CD36* showed large overall donor heterogeneity (Supplementary Fig. S8) in comparison to the macrophage 3D culture.

Discussion

The goal of this study was to fundamentally explore the effects of hyperglycemia, as one of the hallmarks of diabetes, on the macrophage response to electrospun PCL-BU, an often used synthetic biomaterial for *in situ* tissue engineering. Although several studies describe the *in vitro* response of primary human macrophages to synthetic biomaterials (e.g., cells from healthy versus obese donors[52] or macrophages in combination with fibroblasts and/or mesenchymal stromal cells on scaffolds[53]), to the best of our knowledge, no published studies assess the effect of hyperglycemic and hyperosmotic conditions on macrophages in 3D synthetic scaffolds.

Overall, both hyperglycemia and hyperosmotic pressure tended to lead to a general increase in pro-inflammatory

cytokine expression in 2D, and in 3D scaffolds, although the extent of regulation was strongly dependent on the culturing conditions and subject to donor-to-donor variability. Macrophages in 3D co-culture with (myo)fibroblasts in hyperglycemia resulted in an increase in typical (myo)fibroblast activation markers, including *ACTA2*, *COL1A2*, *COL3A1*, as well as *IL-1β* expression and secretion of IL-6. Two particularly striking observations were evident from these results: (1) The observed effects in macrophage response in hyperglycemic conditions were often accompanied by a parallel trend in the hyperosmotic control, and (2) there was a strong donor heterogeneity in the effect of hyperglycemia on macrophage behavior.

Previous studies have assessed the macrophage response in hyperglycemic conditions in terms of macrophage polarization and cytokine secretion, particularly in the (clinical) context of increased susceptibility to infection and poor wound healing in diabetic patients.[54] These studies show a very broad range of experimental study designs, with different cell sources (e.g., human cell lines THP1,[39,55] U937,[40,56] murine cell line RAW 264.7[57,58] or primary human (either diabetic or non-diabetic donors) macrophages[35–37,59] or murine macrophages[60,61]), different definitions of hyperglycemic conditions (ranging from 15 mM glucose[39] up to 44 mM glucose[62]), with[35,39] or without[40,56,59] OC, various stimuli (e.g., LPS, *Mycobacterium tuberculosis*, IFN-γ, IL-4) and different time points of analysis (from hours to days to weeks), as well as a broad variety of assessed cytokines.

Although it remains difficult to draw overall conclusions from such heterogenous study designs, it seems that there is an overall increase in pro-inflammatory cytokine expression by macrophages in hyperglycemic conditions, especially when chemically stimulated with LPS, an often used golden standard control for M1 polarization, which gives an even more extreme response in hyperglycemic conditions. Similarly, we observed a general increase in pro-inflammatory cytokine expression in hyperglycemic conditions in 2D and 3D.

Although a relatively large heterogeneity between the different donors was observed, pro-inflammatory cytokines TNF-α and IL-1β, as well as anti-inflammatory IL-10 seemed to be influenced by hyperglycemic conditions. These findings are similar to previous studies.[35,39] However, we often observed a parallel trend in the OC group too, indicating that the effects are not solely dependent on increased glucose but also due to the elevated osmotic pressure, an observation that has also been reported earlier.[35]

Only very few studies specifically describe the effect of osmotic pressure on macrophages. Ip and Medzhitov exposed murine macrophages to hypertonic conditions (0.2 milli-osmolarity). As expected, an acute shrinkage of the cell was observed within 60 s after exposure to these hypertonic conditions, but this was restored again after 30 min. Next to the morphologic observations, the study showed that in response to hyperosmotic conditions, the macrophages activated caspase-1 in the inflammasome complex, leading to the secretion of IL-1β.[63] Almost two decades earlier, Shapiro and Dinarello analyzed hPBMCs in hyperosmotic stress (305 mOsm) and also found increased production of IL-1β.[64] Although the hyperosmotic stresses in our study were lower, we did observe clear effects of hyperosmotic conditions (both 25 mM glucose and OC group) on *IL-1β* gene expression. Given the limited prior data available on the effect of hyperosmotic pressure and the unexpectedly strong effect of hyperosmotic pressure as observed in this study, these findings warrant a more thorough investigation of the influence of osmotic pressure on the macrophage response to biomaterials, especially considering that skewed osmotic pressure is of clinical relevance in diabetic patients.[65]

Besides the assessment of macrophage response in hyperglycemic conditions in terms of phenotypic markers and inflammatory cytokine response in 2D, we also assessed its effects on ECM remodeling cytokines and in combination with fibroblasts on ECM deposition on a synthetic biomaterial in 3D. The latter is important from an *in situ* tissue engineering perspective. In comparison to the well-defined biochemically induced phenotypes, the macrophages activated by the 3D scaffold generally attain a mixed phenotype, with increased expression of *CD206* and *TNF-α* in hyperosmotic conditions, similar to what we observed in 2D hyperglycemic conditions. Co-culture of monocyte-derived macrophages and (myo)fibroblasts on scaffolds in hyperglycemic conditions resulted in a slightly increased pro-inflammatory environment with increased collagen gene expression levels. This did not translate into differences in tissue production at the protein level, although this is likely influenced by the relatively short culture period.

In addition to phenotypical characterization and cytokine secretion of the macrophages, we measured the expression of the metabolic receptors *CD36* and *SCL2A1* throughout this study. This was motivated by the notion that macrophages prefer specific pathways for their energy production, matching their functional requirements.[29,66–69] Since the pro-inflammatory M1 macrophages belong to the first line of defense, and need to act quick within the first hours to days, they mainly use glucose as a quick energy source. The more regenerative M2 macrophages rely on fatty acid metabolism, which provides a more sustainable supply of energy.[29,66] The first studies reporting on monocyte and macrophage energy consumption showed that (LPS-stimulated) M1 macrophages mainly use glucose as their primary energy source, increase the expression of glucose transporter-1,[70] and shift to aerobic glycolysis, even in the presence of normoxia, also known as the ''Warbug effect.''[71] Contrary, IL-4 stimulated M2 macrophages mainly use fatty acids for which they increase the expression of *CD36* and lipoprotein lipase and rely on mitochondrial oxidative phosphorylation.[72,73]

In accordance with these previous reports, in our study, M1 macrophages showed a higher *SCL2A1* gene expression compared with unpolarized M0 and M2 polarized macrophages,[67,74] and *CD36* was higher expressed in unpolarized and M2 polarized macrophages compared with M1 polarized macrophages.[75,76]

We detected that the expression of both *CD36* and *SCL2A1* at the gene level increased in hyperglycemic and hyperosmotic conditions compared with normoglycemic conditions in both 2D and 3D for all biochemically induced polarization states. This was also observed in 3D for *CD36* expression, whereas *SCL2A1* expression on the other hand displayed a decreased expression in 3D scaffolds when exposed to hyperglycemic conditions. Only a few studies report the direct effect of a hyperglycemic environment on monocyte and macrophage metabolism. A recent study by

Pavlou et al investigated the effect of hyperglycemia on murine bone marrow cell proliferation and differentiation into macrophages.[61]

They showed that sustained high glucose appeared to reduce glycolytic capacity and glycolytic reserve, which resulted in lower levels of NO production and reduced bactericidal activity and ROS production.[61] Edgar et al were triggered by the clinical observation that despite glucose-lowering therapies, diabetic patients remain at elevated risks for cardiovascular complications. The authors hypothesized that hyperglycemia induced trained immunity (long-term innate immune cell memory) in macrophages through epigenetic modifications. Through extensive metabolome, transcriptome, and epigenomic analysis in experiments with both murine and human macrophages, the study demonstrated that, indeed, hyperglycemia induces trained immunity in hematopoietic stem cells (macrophage precursors) and macrophages, due to aerobic glycation, which results in a proinflammatory primed state.[77] It should be noted that our *CD36* and *SCL2A1* results on the gene level may not necessarily translate to protein expression, nor do they provide functional information, such as glucose uptake. Macrophage metabolism is highly complex and given that our focus lies on *in situ* tissue engineering, unraveling the exact mechanisms of macrophage metabolism under the different conditions is beyond the scope of the current study.

With recent advances in the field of immunometabolism, the complexity of macrophage metabolism begins to unveil itself, for which the reader is referred to in-depth reviews by O'Neill et al[68] and Liu et al[71] Follow-up studies that would help in understanding the effect of hyperglycemia on *in situ* tissue engineering may include a more in-depth analysis of metabolic downstream pathways and energy consumption (e.g., via Seahorse real-time ATP assays), or epigenetic analysis to shed light on the metabolic memory of macrophages.[77,78]

The donor heterogeneity as observed in our study can be seen as both a strength and a limitation. The use of primary cells represents the natural variation[79] and physiological conditions better than cell lines. However, when using primary cells from buffy coats, the available number of cells per donor is limited, resulting in a relatively low overall *n* when performing this set of experiments. Next to the limited number of cells, also the available donor information is limited, apart from the sex, age, and blood type of donors, given that the donors are anonymized. Important to note is that in The Netherlands, also diabetic patients can donate blood, provided that they meet certain requirements (e.g., regulated blood sugar levels), which could substantially influence the results of this study.

In 2019, Alrdahe et al compared monocyte-derived macrophages isolated from blood donated by healthy and diabetic volunteers. They demonstrated that classical activation of macrophages from diabetic donors resulted in an increased production of inflammatory cytokines compared with healthy macrophages. Further, macrophages derived from diabetic donors showed impaired maturation.[80] This could be caused by metabolic memory, which is the effect of hyperglycemia causing epigenetic changes in macrophages that promote their pro-inflammatory activation.[81]

Therefore, it remains to be elucidated whether hyperglycemia alone induces the same changes in cells from healthy donors as from diabetic donors, to determine whether exposing healthy cells to a ''diseased'' environment is a relevant model.

This study has several limitations. Due the limited number of macrophages per buffy coat, we were limited in the possible experimental set-ups. When more donors would be incorporated in follow-up studies, it may be possible to delineate cohort-like response profiles to find possible underlying relationships within the variance. Although hyperglycemia is one of the major hallmarks of diabetes, other systemic metabolic conditions, such as hyperinsulinemia or the aggressive oxidative environment, hamper immune cell function and regenerative capacity in these patients.[27] Finally, diabetic patients are most often pharmacologically treated, the influence of these medications might have an impact too on the macrophage function, but these were not taken into account in this study.

Conclusion

In summary, this observative study shows that primary human macrophages are sensitive to hyperglycemia and that this affects the macrophage response to a 3D electrospun scaffold. Much of these effects may be at least partly attributed to the hyperosmotic environment that is caused by the elevated glucose levels. Moreover, this study emphasizes the importance of donor-to-donor variability, which highlights the need to study such phenomena with primary human cells. To the best of our knowledge, this is the first study to explore the influence of hyperglycemia on the macrophage response to 3D scaffold and our findings are an initial step toward developing more predictive models to unravel macrophage-driven *in situ* tissue engineering.

Acknowledgments

The authors thank Wochiech Szymchyk for electrospinning of the PCL-BU scaffold and Sylvia Dekker for her help with optimization of the stainings.

Authors' Contributions

Conceptualization: S.E.K. and A.I.P.M.S.; experimental work: F.L.P.V., S.S., and S.E.K.; formal analysis: S.E.K., F.L.P.V., S.S., and A.I.P.M.S.; writing-original draft preparation: S.E.K., F.L.P.V., and S.S.; writing—review and editing: A.I.P.M.S., S.M.M., and C.V.C.B.; supervision: A.I.P.M.S. and C.V.C.B.; and funding acquisition: C.V.C.B. All authors have read and agreed to the published version of the article.

Disclosure Statement

No competing financial interests exist.

Funding Information

This study was financially supported by the InSiTeVx project (Grant No. 436001003), which is financially supported by ZonMw within the LSH 2Treat Programme and the Dutch Kidney Foundation. The Gravitation Program ''Materials Driven Regeneration'' was funded by the Netherlands Organization for Scientific Research (Grant No. 024.003.013).

Supplementary Material

Supplementary Data
Supplementary Figure S1
Supplementary Figure S2
Supplementary Figure S3
Supplementary Figure S4
Supplementary Figure S5
Supplementary Figure S6
Supplementary Figure S7
Supplementary Figure S8
Supplementary Table S1
Supplementary Table S2
Supplementary Table S3
Supplementary Table S4

References

1. Gao J, Jiang L, Liang Q, et al. The grafts modified by heparinization and catalytic nitric oxide generation used for vascular implantation in rats. Regen Biomater 2018;5(2): 105–114; doi: 10.1093/rb/rby003.
2. Khosravi R, Best CA, Allen RA, et al. Long-term functional efficacy of a novel electrospun poly(glycerol sebacate)-based arterial graft in mice. Ann Biomed Eng 2016;44(8):2402–2416; doi: 10.1007/s10439-015-1545-7.
3. Matsumura G, Isayama N, Matsuda S, et al. Long-term results of cell-free biodegradable scaffolds for in situ tissue engineering of pulmonary artery in a canine model. Biomaterials 2013;34(27):6422–6428; doi: http://dx.doi.org/10.1016/j.biomaterials.2013.05.037.
4. Bonito V, Koch SE, Krebber MM, et al. distinct effects of heparin and interleukin-4 functionalization on macrophage polarization and in situ arterial tissue regeneration using resorbable supramolecular vascular grafts in rats. Adv Healthc Mater 2021;10(21):2101103; doi: 10.1002/adhm.202101103.
5. Kluin J, Talacua H, Smits AIP, et al. In situ heart valve tissue engineering using a bioresorbable elastomeric implant from material design to 12 months follow-up in sheep. Biomaterials 2017;125:101–117; doi: 10.1016/j.biomaterials.2017.02.007.
6. Fioretta ES, Lintas V, Mallone A, et al. differential leaflet remodeling of bone marrow cell pre-seeded versus non-seeded bioresorbable transcatheter pulmonary valve replacements. JACC Basic to Transl Sci 2020;5(1):15–31; doi: 10.1016/j.jacbts.2019.09.008.
7. Uiterwijk M, Smits AIPM, van Geemen D, et al. In situ remodeling overrules bioinspired scaffold architecture of supramolecular elastomeric tissue-engineered heart valves. JACC Basic to Transl Sci 2020;5(12):1187–1206; doi: 10.1016/j.jacbts.2020.09.011.
8. Mori da Cunha MGMC, Arts B, Hympanova L, et al. Functional supramolecular bioactivated electrospun mesh improves tissue ingrowth in experimental abdominal wall reconstruction in rats. Acta Biomater 2020;106:82–91; doi: 10.1016/j.actbio.2020.01.041.
9. Hibino N, McGillicuddy E, Matsumura G, et al. Late-term results of tissue-engineered vascular grafts in humans. J Thorac Cardiovasc Surg 2010;139(2):431–436.e2; doi: 10.1016/j.jtcvs.2009.09.057.
10. Drews JD, Pepper VK, Best CA, et al. Spontaneous reversal of stenosis in tissue-engineered vascular grafts. Sci Transl Med 2020;12(537):eaax6919; doi: 10.1126/scitranslmed.aax6919.
11. Morales DL, Herrington C, Bacha EA, et al. A novel restorative pulmonary valve conduit: early outcomes of two clinical trials. Front Cardiovasc Med 2021;7; doi: 10.3389/fcvm.2020.583360.
12. Wissing TB, Bonito V, Bouten CVC, et al. Biomaterial-driven in situ cardiovascular tissue engineering—a multi-disciplinary perspective. NPJ Regen Med 2017;2(1):18; doi: 10.1038/s41536-017-0023-2.
13. Talacua H, Smits AIP., Muylaert DEP, et al. In situ tissue engineering of functional small-diameter blood vessels by host circulating cells only. Tissue Eng Part A 2015;21(19–20):2583–2594; doi: 10.1089/ten.tea.2015.0066.
14. Mosser DM, Edwards JP. Exploring the full spectrum of macrophage activation. Nat Rev Immunol 2008;8(12):958–969; doi: 10.1038/nri2448.Exploring.
15. Witherel CE, Abebayehu D, Barker TH, et al. Macrophage and fibroblast interactions in biomaterial-mediated fibrosis. Adv Healthc Mater 2019;1801451:1801451; doi: 10.1002/adhm.201801451.
16. Ogle ME, Segar CE, Sridhar S, et al. Monocytes and macrophages in tissue repair: implications for immunoregenerative biomaterial design. Exp Biol Med 2016;241(10):1084–1097; doi: 10.1177/1535370216650293.
17. Spiller KL, Anfang RR, Spiller KJ, et al. The role of macrophage phenotype in vascularization of tissue engineering scaffolds. Biomaterials 2014;35(15):4477–4488; doi: 10.1016/j.biomaterials.2014.02.012.
18. Smits AIPM, Bouten CVC. Tissue engineering meets immunoengineering: prospective on personalized in situ tissue engineering strategies. Curr Opin Biomed Eng 2018;6:17–26; doi: 10.1016/j.cobme.2018.02.006.
19. de Kort BJ, Koch SE, Wissing TB, et al. Immunoregenerative biomaterials for in situ cardiovascular tissue engineering: Do patient characteristics warrant precision engineering? Adv Drug Deliv Rev 2021;178:113960; doi: 10.1016/j.addr.2021.113960.
20. IDF. International Diabetes Federation: Diabetes Atlas 9th Edition. 2019. Available from: https://diabetesatlas.org/data/en/world/ [Last accessed: 10/12/2021].
21. Negre-Salvayre A, Salvayre R, Augé N, et al. Hyperglycemia and glycation in diabetic complications. Antioxidants Redox Signal 2009;11(12):3071–3109; doi: 10.1089/ars.2009.2484.
22. Beckman JA, Creager MA. Vascular complications of diabetes. Circ Res 2016;118(11):1771–1785; doi: 10.1161/CIRCRESAHA.115.306884.
23. Kogan A, Ram E, Levin S, et al. Impact of type 2 diabetes mellitus on short- and long-term mortality after coronary artery bypass surgery. Cardiovasc Diabetol 2018;17(1):1–8; doi: 10.1186/s12933-018-0796-7.
24. Mathew V, Gersh BJ, Williams BA, et al. Outcomes in patients with diabetes mellitus undergoing percutaneous coronary intervention in the current era: A report from the Prevention of REStenosis with Tranilast and Its Outcomes (PRESTO) Trial. Circulation 2004;109(4):476–480; doi: 10.1161/01.CIR.0000109693.64957.20.
25. Gilbert J, Raboud J, Zinman B. Meta-analysis of the effect of diabetes on restenosis rates among patients receiving coronary angioplasty stenting. Diabetes Care 2004;27(4):990–994; doi: 10.2337/diacare.27.4.990.
26. Lin MJ, Chang YJ, Chen CY, et al. Influence of hypercholesterolemia and diabetes on long-term outcome in patients with stable coronary artery disease receiving percutaneous coronary intervention. Medicine (Baltimore) 2019;98(34):e16927; doi: 10.1097/MD.0000000000016927.

27. Dhulekar J, Simionescu A. Challenges in vascular tissue engineering for diabetic patients. Acta Biomater 2018;70: 25–34; doi: 10.1016/j.actbio.2018.01.008.
28. Meshkani R, Vakili S. Tissue resident macrophages: key players in the pathogenesis of type 2 diabetes and its complications. Clin Chim Acta 2016;462:77–89; doi: 10.1016/j.cca.2016.08.015.
29. Shapouri-Moghaddam A, Mohammadian S, Vazini H, et al. Macrophage plasticity, polarization, and function in health and disease. J Cell Physiol 2018;233(9):6425–6440; doi: 10.1002/jcp.26429.
30. Gupta S, Koirala J, Khardori R, et al. Infections in diabetes mellitus and hyperglycemia. Infect Dis Clin North Am 2007;21(3):617–638; doi: 10.1016/j.idc.2007.07.003.
31. Zheng W, Wang Z, Song L, et al. Endothelialization and patency of RGD-functionalized vascular grafts in a rabbit carotid artery model. Biomaterials 2012;33(10):2880–2891; doi: 10.1016/j.biomaterials.2011.12.047.
32. Wang Z, Zheng W, Wu Y, et al. Differences in the performance of pcl-based vascular grafts as abdominal aorta substitutes in healthy and diabetic rats. Biomater Sci 2016;4(10):1485–1492; doi: http://dx.doi.org/10.1039/c6bm00178e.
33. Chow JP, Simionescu DT, Carter AL, et al. Immunomodulatory effects of adipose tissue-derived stem cells on elastin scaffold remodeling in diabetes. Tissue Eng Regen Med 2016;13(6):701–712; doi: http://dx.doi.org/10.1007/s13770-016-0018-x.
34. Socarrás TO, Vasconcelos AC, Campos PP, et al. Foreign body response to subcutaneous implants in diabetic rats. PLoS One 2014;9(11):e110945; doi: 10.1371/journal.pone.0110945.
35. Lachmandas E, Vrieling F, Wilson LG, et al. The effect of hyperglycaemia on in vitro cytokine production and macrophage infection with *Mycobacterium tuberculosis*. PLoS One 2015;10(2):1–13; doi: 10.1371/journal.pone.0117941.
36. Moganti K, Li F, Schmuttermaier C, et al. Hyperglycemia induces mixed M1/M2 cytokine profile in primary human monocyte-derived macrophages. Immunobiology 2017;222(10):952–959; doi: 10.1016/j.imbio.2016.07.006.
37. Torres-Castro I, Arroyo-Camarena ÚD, Martínez-Reyes CP, et al. Human monocytes and macrophages undergo m1-type inflammatory polarization in response to high levels of glucose. Immunol Lett 2016;176:81–89; doi: 10.1016/j.imlet.2016.06.001.
38. Fadini GP, De Kreutzenberg SV, Boscaro E, et al. An unbalanced monocyte polarisation in peripheral blood and bone marrow of patients with type 2 diabetes has an impact on microangiopathy. Diabetologia 2013;56(8):1856–1866; doi: 10.1007/s00125-013-2918-9.
39. Grosick R, Alvarado-Vazquez PA, Messersmith AR, et al. High glucose induces a priming effect in macrophages and exacerbates the production of pro-inflammatory cytokines after a challenge. J Pain Res 2018;11:1769–1778; doi: 10.2147/JPR.S164493.
40. Maldonado A, He L, Game BA, et al. Pre-exposure to high glucose augments lipopolysaccharide-stimulated matrix metalloproteinase-1 expression by human U937 histiocytes. J Periodontal Res 2004;39(6):415–423; doi: 10.1111/j.1600-0765.2004.00756.x.
41. Louiselle AE, Niemiec SM, Zgheib C, et al. Macrophage polarization and diabetic wound healing. Transl Res 2021;236:109–116; doi: 10.1016/j.trsl.2021.05.006.
42. Kimball AS, Davis FM, denDekker A, et al. The histone methyltransferase setdb2 modulates macrophage phenotype and uric acid production in diabetic wound repair. Immunity 2019;51(2):258–271.e5; doi: 10.1016/j.immuni.2019.06.015.
43. Tiemeijer BM, Sweep MWD, Sleeboom JJF, et al. Probing single-cell macrophage polarization and heterogeneity using thermo-reversible hydrogels in droplet-based microfluidics. Front Bioeng Biotechnol 2021;9(October):1–14; doi: 10.3389/fbioe.2021.715408.
44. Madonna R, Geng Y-J, Shelat H, et al. High glucose-induced hyperosmolarity impacts proliferation, cytoskeleton remodeling and migration of human induced pluripotent stem cells via Aquaporin-1. Biochim Biophys Acta Mol Basis Dis 2014;1842(11):2266–2275; doi: 10.1016/j.bbadis.2014.07.030.
45. Schnell AM, Hoerstrup SP, Zund G, et al. Optimal cell source for cardiovascular tissue engineering: Venous vs. aortic human myofibroblasts. Thorac Cardiovasc Surg 2001;49(4):221–225; doi: 10.1055/s-2001-16113.
46. Vogel DYS, Glim JE, Stavenuiter AWD, et al. Human macrophage polarization in vitro: maturation and activation methods compared. Immunobiology 2014;219(9):695–703; doi: 10.1016/j.imbio.2014.05.002.
47. Mol A, Van Lieshout MI, Dam-De Veen CG, et al. Fibrin as a cell carrier in cardiovascular tissue engineering applications. Biomaterials 2005;26(16):3113–3121; doi: 10.1016/j.biomaterials.2004.08.007.
48. Koch SE, van Haaften EE, Wissing TB, et al. A multi-cue bioreactor to evaluate the inflammatory and regenerative capacity of biomaterials under flow and stretch. J Vis Exp 2020;(166):1–32; doi: 10.3791/61824.
49. Wissing TB, van Haaften EE, Koch SE, et al. Hemodynamic loads distinctively impact the secretory profile of biomaterial-activated macrophages: Implications for in situ vascular tissue engineering. Biomater Sci 2020;8(1):132–147; doi: 10.1039/C9BM01005J.
50. Grotenhuis N, Bayon Y, Lange JF, et al. A culture model to analyze the acute biomaterial-dependent reaction of human primary macrophages. Biochem Biophys Res Commun 2013;433(1):115–120; doi: 10.1016/j.bbrc.2013.02.054.
51. Boerboom RA, Nash K, Megens RTA, et al. High resolution imaging of collagen organisation and synthesis using a versatile collagen specific probe. 2007;159:392–399; doi: 10.1016/j.jsb.2007.04.008.
52. Boersema GSA, Utomo L, Bayon Y, et al. Monocyte subsets in blood correlate with obesity related response of macrophages to biomaterials in vitro. Biomaterials 2016;109:32–39; doi: 10.1016/j.biomaterials.2016.09.009.
53. Caires HR, Barros da Silva P, Barbosa MA, et al. A co-culture system with three different primary human cell populations reveals that biomaterials and MSC modulate macrophage-driven fibroblast recruitment. J Tissue Eng Regen Med 2018;12(3):e1433–e1440; doi: 10.1002/term.2560.
54. Baltzis D, Eleftheriadou I, Veves A. Pathogenesis and treatment of impaired wound healing in diabetes mellitus: New Insights. Adv Ther 2014;31(8):817–836; doi: 10.1007/s12325-014-0140-x.
55. Morey M, O'Gaora P, Pandit A, et al. Hyperglycemia acts in synergy with hypoxia to maintain the pro-inflammatory phenotype of macrophages. PLoS One 2019;14(8):e0220577; doi: 10.1371/journal.pone.0220577.

56. Nareika A, Sundararaj KP, Im Y Bin, et al. High glucose and interferon gamma synergistically stimulate MMP-1 expression in U937 macrophages by increasing transcription factor STAT1 activity. Atherosclerosis 2009;202(2):363–371; doi: 10.1016/j.atherosclerosis.2008.05.043.
57. Kurihara C, Tanaka T, Yamanouchi D. Hyperglycemia attenuates receptor activator of nf-κb ligand–induced macrophage activation by suppressing insulin signaling. J Surg Res 2017;214:168–175; doi: 10.1016/j.jss.2017.02.009.
58. Wang J, Liu J, Wang Y, et al. High glucose induces alternative activation of macrophages via PI3K/Akt signaling pathway. J Recept Signal Transduct 2017;37(4):409–415; doi: 10.1080/10799893.2017.1298131.
59. Vance J, Santos A, Sadofsky L, et al. Effect of high glucose on human alveolar macrophage phenotype and phagocytosis of mycobacteria. Lung 2019;197(1):89–94; doi: 10.1007/s00408-018-0181-z.
60. Ayala TS, Tessaro FHG, Jannuzzi GP, et al. High glucose environments interfere with bone marrow-derived macrophage inflammatory mediator release, the TLR4 pathway and glucose metabolism. Sci Rep 2019;9(1):1–15; doi: 10.1038/s41598-019-47836-8.
61. Pavlou S, Lindsay J, Ingram R, et al. Sustained high glucose exposure sensitizes macrophage responses to cytokine stimuli but reduces their phagocytic activity. BMC Immunol 2018;19(1):1–13; doi: 10.1186/s12865-018-0261-0.
62. Sun C, Sun L, Ma H, et al. The phenotype and functional alterations of macrophages in mice with hyperglycemia for long term. J Cell Physiol 2012;227(4):1670–1679; doi: 10.1002/jcp.22891.
63. Ip WKE, Medzhitov R. Macrophages monitor tissue osmolarity and induce inflammatory response through NLRP3 and NLRC4 inflammasome activation. Nat Commun 2015;6(1):6931; doi: 10.1038/ncomms7931.
64. Shapiro L, Dinarello CA. Hyperosmotic stress as a stimulant for proinflammatory cytokine production. Exp Cell Res 1997;231(2):354–362; doi: 10.1006/excr.1997.3476.
65. Pasquel FJ, Umpierrez GE. Hyperosmolar hyperglycemic state: A historic review of the clinical presentation, diagnosis, and treatment. Diabetes Care 2014;37(11):3124–3131; doi: 10.2337/dc14-0984.
66. Galván-Peña S, O'Neill LAJ. Metabolic reprogramming in macrophage polarization. Front Immunol 2014;5(AUG):1–6; doi: 10.3389/fimmu.2014.00420.
67. Geeraerts X, Bolli E, Fendt SM, et al. Macrophage metabolism as therapeutic target for cancer, atherosclerosis, and obesity. Front Immunol 2017;8(March); doi: 10.3389/fimmu.2017.00289.
68. O'Neill LAJ, Kishton RJ, Rathmell J. A Guide to immunometabolism for immunologists. Nat Rev Immunol 2016;16(9):553–565; doi: 10.1038/nri.2016.70.
69. Caputa G, Flachsmann LJ, Cameron AM. Macrophage metabolism: A wound-healing perspective. Immunol Cell Biol 2019;97(3):268–278; doi: 10.1111/imcb.12237.
70. Fukuzumi M, Shinomiya H, Shimizu Y, et al. Endotoxin-induced enhancement of glucose influx into murine peritoneal macrophages via GLUT 1. Infect Immun 1996;64(1):108–112; doi: 10.1128/iai.64.1.108-112.1996.
71. Liu Y, Xu R, Gu H, et al. Metabolic reprogramming in macrophage responses. Biomark Res 2021;9(1):1–17; doi: 10.1186/s40364-020-00251-y.
72. Vats D, Mukundan L, Odegaard JI, et al. Oxidative metabolism and PGC-1β attenuate macrophage-mediated inflammation. Cell Metab 2006;4(1):13–24; doi: 10.1016/j.cmet.2006.05.011.
73. Langston PK, Shibata M, Horng T. Metabolism supports macrophage activation. Front Immunol 2017;8(JAN):1–7; doi: 10.3389/fimmu.2017.00061.
74. Jung J, Zeng H, Horng T. Metabolism as a Guiding Force for Immunity. Nat Cell Biol 2019;21(1):85–93; doi: 10.1038/s41556-018-0217-x.
75. Viola A, Munari F, Sánchez-Rodríguez R, et al. The metabolic signature of macrophage responses. Front Immunol 2019;10(JULY):1–16; doi: 10.3389/fimmu.2019.01462.
76. Rosa Neto JC, Calder PC, Curi R, et al. The immunometabolic roles of various fatty acids in macrophages and lymphocytes. Int J Mol Sci 2021;22(16):8460; doi: 10.3390/ijms22168460.
77. Edgar L, Akbar N, Braithwaite AT, et al. Hyperglycemia induces trained immunity in macrophages and their precursors and promotes atherosclerosis. Circulation 2021;961–982; doi: 10.1161/CIRCULATIONAHA.120.046464.
78. Logie C, Stunnenberg HG. Epigenetic memory: A macrophage perspective. Semin Immunol 2016;28(4):359–367; doi: 10.1016/j.smim.2016.06.003.
79. Eady JJ, Wortley GM, Wormstone YM, et al. Variation in gene expression profiles of peripheral blood mononuclear cells from healthy volunteers. Physiol Genomics 2005;22:402–411; doi: 10.1152/physiolgenomics.00080.2005.
80. Alrdahe S, Al Sadoun H, Torbica T, et al. Dysregulation of macrophage development and phenotype in diabetic human macrophages can be rescued by Hoxa3 protein transduction. PLoS One 2019;14(10):1–26; doi: 10.1371/journal.pone.0223980.
81. Ahmed M, de Winther MPJ, Van den Bossche J. Epigenetic mechanisms of macrophage activation in type 2 diabetes. Immunobiology 2017;222(10):937–943; doi: 10.1016/j.imbio.2016.08.011.

Address correspondence to:
Anthal I.P.M. Smits, PhD
Department of Biomedical Engineering
Eindhoven University of Technology
Den Dolech 2
Gemini-Zuid 4.106
Eindhoven 5612AZ
The Netherlands

E-mail: a.i.p.m.smits@tue.nl

Received: April 11, 2022
Accepted: June 1, 2022
Online Publication Date: July 13, 2022